

XMM-Newton observations of the supernova remnant RX J0852.0-4622 / GRO J0852-4642

A. F. Iyudin, B. Aschenbach, W. Becker, K. Dennerl, F. Haberl

Max-Planck-Institut für extraterrestrische Physik, 85741 Garching, Germany

Received ...; Accepted ...

Abstract. RX J0852.0-4622 is a supernova remnant discovered in the *ROSAT* all-sky survey. Spatially coincident 1.157 MeV γ -ray line emission was detected with the *COMPTEL* instrument on-board of the CGRO. The analysis combining the X-ray and γ -ray data suggests that RX J0852.0-4622 is a close-by and young supernova remnant. Follow-up observations with *ASCA* show that the two brightest sections of the limb have non-thermal spectra, which make an independent assessment of the age and distance using the Sedov equations for the evolution of the remnant almost impossible. We have observed three rim sections of RX J0852.0-4622 with *XMM-Newton* and confirm the power law type spectra measured with *ASCA*. We also confirm the presence of an emission line like feature at 4.45 ± 0.05 keV, which we suggest to be emission from Ti and Sc excited by atom/ion or ion/ion high velocity collisions. The high velocity is in agreement with the width of the 1.157 MeV γ -ray line. The X-ray line flux expected from such an interaction is consistent with the 1.157 MeV γ -ray line flux measured by *COMPTEL*. This consistency of the X-ray line flux and the γ -ray line flux lends further support to the existence and amounts of Ti in RX J0852.0-4622 claimed by Iyudin et al. (1998) and to the suggestion that RX J0852.0-4622 is young and nearby (Aschenbach et al. 1999). Iyudin et al. (1998) quote a very large broadening of the 1.157 MeV γ -ray line which would indicate a large velocity of the emitting matter of about 15.000 km/s. Such high ejecta velocity for Ti is found only in explosion models of sub-Chandrasekhar type Ia supernovae (Woosley & Weaver 1994, Livne & Arnett 1995). In this case no compact remnant is expected. The obvious questions remaining are what the nature and the origin of the central compact source CXOU J085201.4-461753 are and why the absorption column density apparently associated with RX J0852.0-4622 is much greater than the typical column for the Vela SNR.

Key words. – processes: nucleosynthesis – supernovae: general – ISM: individual: RX J0852.0-4622 – ISM: supernova remnants – Gamma-rays: observation – X-rays: ISM

1. Introduction

The *ROSAT* all-sky survey has revealed a number of previously unknown supernova remnants (SNR) among which is RX J0852.0-4622, sometimes referred to as G266.2-1.2, which is located at the south-eastern corner of the Vela SNR (Aschenbach 1998). The all-sky map of ~ 6 years of *COMPTEL* data shows a few localized 1.157 MeV line emission features. This γ -ray line originates from the decay of radioactive ^{44}Ti (Iyudin et al. 1998, Iyudin 1999). The most significant excess is attributed to the Cas A SNR whereas the second brightest structure called GRO J0852-4642 coincides with RX J0852.0-4622 (Iyudin 1999, Iyudin et al. 1998). Since ^{44}Ti is exclusively produced in supernovae it is very likely that RX J0852.0-4622 and GRO J0852-4642 are the same object which was created in one supernova explosion. The combined analysis of the X-ray data and the γ -ray data led to the suggestion that RX J0852.0-4622 could be the remnant of the nearest supernova in recent history (Aschenbach et al. 1999) with a best

estimate for the distance of 200 pc and an age of 680 years. The detection of the 1.157 MeV γ -ray line from radioactive ^{44}Ti in Cas A (Iyudin et al. 1994, 1997) has been supported by the *Beppo-SAX* measurements of the ~ 68 and ~ 78 keV X-ray lines (Vink et al. 2001) which are produced in the first decay of ^{44}Ti in the decay chain $^{44}\text{Ti} \rightarrow ^{44}\text{Sc} \rightarrow ^{44}\text{Ca}$. The detection of the 1.157 MeV γ -ray line from Cas A was the first discovery of ^{44}Ti in a young galactic SNR, and as such it provides an essential calibration of nucleosynthesis model calculations. With the discovery of RX J0852.0-4622/GRO J0852-4642 we may have a second example.

Follow-up observations in the radio band confirmed the shell-like structure and supported the identification of RX J0852.0-4622 as a SNR (Combi et al. 1999, Duncan and Green 2000, Filipovic 2001). Furthermore a good correlation between X-ray and radio brightness was found (c.f. Fig. 1, Filipovic 2001).

The spectra taken with *ROSAT* are compatible with either emission from a high temperature plasma or a non-thermal source creating a power law (Aschenbach et al. 1999). The X-ray surface brightness of RX J0852.0-4622 is generally low and

Send offprint requests to: A. F. Iyudin
(aiyudin@srd.sinp.msu.ru)

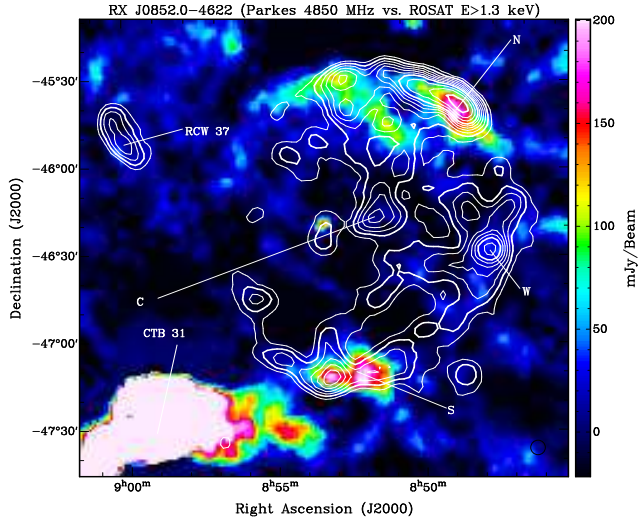


Fig. 1. The Parkes image (colour) of RX J0852.0-4622 overlaid with ROSAT PSPC contours ($E > 1.3$ keV). The synthesized beam of the Parkes observations is $5'$ (lower left corner) with an r.m.s noise (1σ) of 10 mJy. X-ray contours (white) are 0.8, 1, 1.2, 1.4, 1.6, 1.8, 2, 2.3, 2.6 and 3 in units of 10^{-4} ROSAT PSPC counts s^{-1} arcmin $^{-2}$ (Filipovic 2001).

implies a rather low matter density for any shock wave heated plasma. Follow up measurements with *ASCA* in December 1998 generally confirmed the results of *ROSAT* but demonstrated that the spectrum is definitely non-thermal with no obvious emission lines above 1 keV (Tsunemi et al. 2000, Slane et al. 2001). The best-fit with a single power law results in an interstellar absorption column density which is at least a factor of three higher than the highest value observed elsewhere in the Vela SNR (Lu & Aschenbach 2000).

Based on the *ROSAT* data Aschenbach (1998) suggested the presence of a central point source, which later was confirmed by *Chandra* measurements (Pavlov et al. 2001). The spectrum of the source CXOU J085201.4-461753 suggests a neutron star as the emitter (Kargaltsev et al. 2002), which is supported by the absence of any optical counterpart brighter than $B \sim 23$ (Mereghetti et al. 2002). If this object is the compact remnant of the supernova which created RX J0852.0-4622 the supernova was of the core-collapse type. Like for the north-western rim the absorbing column density inferred from the spectrum of CXOU J085201.4-461753 is significantly higher by a factor of about six (Kargaltsev et al. 2002) than the column densities measured for the Vela SNR (Lu & Aschenbach 2000), which suggests that at least CXOU J085201.4-461753 and possibly RX J0852.0-4622 are at a greater distance than the Vela SNR, which is located at a distance of about 250 pc (Cha et al., 1999). On the other hand, Redman et al. (2002) suggested, as one possibility, that the optical nebula RCW 37 was generated by the blast wave of RX J0852.0-4622 impacting the shell of the Vela SNR, i.e. RX J0852.0-4622 is embedded in the Vela SNR. From observations of 60 O stars Cha & Sembach (2000) have recommended a distance of 390 ± 100 pc to the Vela SNR. Along the line of sight towards the O star HD 75821 (BO IIIIFs at $l, b = 266^\circ.25 / -1^\circ.54$) at a distance of

$\sim 830 \pm 360$ pc absorption lines of Ca II at 3933 \AA and of Na I at 5889 \AA were found. This line of sight is passing through the RX J0852.0-4622 shell near its center. From these observations a distance limit to RX J0852.0-4622 of $\leq 830 \pm 360$ pc can be derived. Pozzo et al. (2000) conclude that the distance to RX J0852.0-4622 is $\approx 430 \pm 60$ pc. From radio observations of the CS $J = 2 - 1$ transitions towards the source G 267.94-1.06, which is at a distance of 700 pc, a cloud was found which has a core mass of $1500 M_\odot$ and an extent of ~ 1.4 pc along the line of sight, or a mean density of 10^4 cm^{-3} of CS (Zinchenko, Mattila and Toriseva, 1995). Deep absorption features in the CO and CS profiles were observed in several sources clustering mainly around $l \approx 270^\circ$. The authors argue that this can be attributed to extended low-excitation foreground clouds. It means that the distance to the south-eastern rim of RX J0852.0-4622 can be < 700 pc. From the observations of the Gum Nebula in the OH line at 1667 MHz the distance to the Vela OB2 association was derived to 420 ± 30 pc (Woermann et al. 2001), which would also be the distance of RX J0852.0-4622 if it would belong to Vela OB2.

Concerning the age, there has been the suggestion, that the supernova which led to RX J0852.0-4622 was responsible for a previously unidentified spike in nitrate concentration measured in an Antarctic ice core. The precipitation occurred around the year 1320. Other nitrate spikes could be associated with historical supernovae (Burgess & Zuber 2000). One of the issues in this context is of course the detection of the 1.157 MeV line, because together with the ^{44}Ti yield it dominates the estimate of the age. There have been numerous discussions about the significance of the 1.157 MeV line (see e.g. Aschenbach et al. 1999, Iyudin 2000, Schönfelder et al. 2000, Iyudin and Aschenbach 2001) and it is obvious that an independent confirmation is needed. First attempts made with *Integral* have so far produced an upper limit, which is about three times as high as the flux measured with *COMPTEL* (von Kienlin et al. 2004).

A totally different explanation for RXJ0852.0-4622 has been given by Wang & Chevalier (2002), who suggest that the ring-like radio and X-ray structure could have been produced by clumps generated in and by the Vela SNR. To shed further light on the questions including distance, age and progenitor we carried out *XMM-Newton* observations of three circular sections distributed along the rim of RX J0852.0-4622 (Fig. 2). The results obtained from the measurements of the central region including the compact source CXOU J085201.4-461753 will be reported elsewhere. The earlier *ASCA* observations were dedicated to study the enhanced X-ray emission regions along the northern and western limbs, the results of which we compare with our findings. We have added an observation of the south-eastern X-ray bright shell section which was not observed by *ASCA* (Tsunemi et al. 2000, Slane et al. 2001). Generally the *ASCA* observations showed that the spectra follow a power law with a photon spectral index of ~ 2.6 and no emission lines have been detected in the GIS spectra (Tsunemi et al. 2000, Slane et al. 2001). But the analysis of the spectra taken with the SIS reveals a line feature at an energy of ~ 4.1 keV in the spectrum of the north-western (NW) rim (Tsunemi et al. 2000). The best-fit model actually consists of two thermal components and an emission line at 4.1 ± 0.2 keV.

This model implies a large overabundance of Ca based on the line flux at 4.1 keV, which was interpreted as the He-like K emission line of ^{44}Ca , which is the final product of the decay of ^{44}Ti (Tsunemi et al. 2000). A feature at 4.1 keV in the SIS0 chip of the *ASCA* detector was also noted by Slane et al. (2001), but the authors were not convinced of its presence because of the low significance. However, if interpreted as the ^{44}Sc -K fluorescence line, the immediate decay product of ^{44}Ti , the upper limit of the Sc flux like the Ca flux is not inconsistent with the flux expected from the ^{44}Ti flux measured by Iyudin et al. (1998). If the X-ray lines are present at a flux level proposed by the observations the age of RXJ0852.0-4622 is not inconsistent with ~ 1000 years (Tsunemi et al. 2000). Previously we have suggested (see Iyudin & Aschenbach, 2001) that a joint analysis of the γ -ray line emission data from radioactive elements in combination with the spatially resolved X-ray spectroscopic data can provide stringent constraints on the abundance of some elements and on the type of the supernova. Here we compare results of the γ -ray data analysis of the SNR RXJ0852.0-4622/GROJ0852-4642 obtained with *COMPTEL* on-board of the Compton Gamma-Ray Observatory (CGRO) with the spatially resolved X-ray spectra obtained with *XMM-Newton*. Specifically, we discuss the X-ray continuum shape at $E_X \geq 1.0$ keV along the X-ray bright rim of the SNR, and the line feature at ~ 4.2 keV. We believe that the X-ray line at ~ 4.2 keV is a direct consequence of the ^{44}Ti decay in SNR shell, which would imply the presence of high-velocity ^{44}Ti in RX J0852.0-4622, and which is suggested by the width of the 1.157 MeV γ -ray line first measured with *COMPTEL* (Iyudin et al. 1998).

2. Observations

The diameter of RX J0852.0-4622 is $\sim 2^\circ$ which is significantly larger than the $\sim 30'$ field of view of the EPIC instruments on board of *XMM-Newton*. Four different pointings on the brightest sections of the remnant were carried out in the GTO program, three of which were directed to the rim, i.e. the northwest (NW), the west (W) and the south (S) and the fourth pointing was towards the center (C) (Fig. 2). The observations were carried out between April 24 and April 27, 2001. The EPIC-PN camera (Strüder et al. 2001) was operated in extended full frame mode and the medium filter was in place. The EPIC-MOS1 and -MOS2 cameras (Turner et al. 2001) were used in full frame mode with the medium filter as well. Further details of the observations are given in Table 1.

3. Spectral fits

RX J0852.0-4622 is located in the south-eastern corner of the Vela SNR, which actually completely covers RX J0852.0-4622. At low energies the X-ray surface brightness of the Vela SNR is much higher than that of RX J0852.0-4622, so that RX J0852.0-4622 becomes visible only above ~ 1 keV in the *ROSAT* images. This is a major complication for any spectral fits to RX J0852.0-4622. We have followed three options. In a first approach we chose fields for the background to be subtracted which are definitely outside the area covered by RX

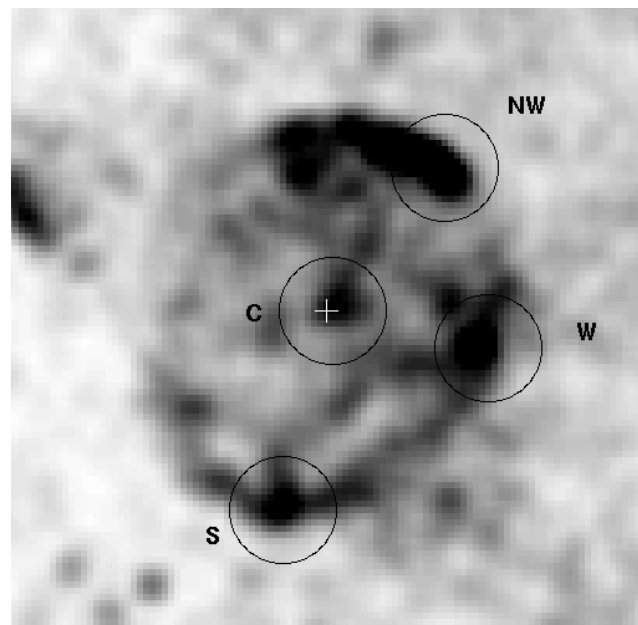


Fig. 2. *ROSAT* grey scale image of RX J0852.0-4622 for $E_x \geq 1.3$ keV; black circles show the *XMM-Newton* GTO fields in the northwest (NW), the west (W), the south (S) and the center (C) of the remnant. North is up and east is to the left. The white cross marks the position of the point source CXOU J085201.4-461753.

J0852.0-4622 but inside the Vela SNR. The corresponding fits did not converge to a unique solution, when different fields for the background were chosen. This is likely to be due to the Vela spectra changing on a scale of a few arcminutes (Lu & Aschenbach 2000). In a second approach we fit the spectra of RX J0852.0-4622 with a three component model. This model consists of one thermal component with an associated interstellar absorption column density which together represent the low energy Vela SNR emission; the second component is again thermal emission with an added power law (third component) to represent the higher energy emission. The second and third components have the same absorption column density. This model was applied to the NW rim and the S rim, and the results are shown in Table 2.

As expected from the work of Lu & Aschenbach (2000) there is a low temperature component (*vmekal1*) with a temperature between 37 and 44 eV associated with a column density around $1.3 \times 10^{21} \text{ cm}^{-2}$, which is about a factor of two to three higher than found by Lu & Aschenbach (2000). But the column density for the high temperature (*vmekal2*)/ power law components is higher by another factor of three to four, which would indicate a larger distance if the spectral model is correct. Formally, i.e. based on χ^2_ν (c.f. Table 2), the fits are acceptable for both the NW and S region, with no significant difference of the best fit parameters for the two regions. The power law slopes of 2.59 and 2.55, respectively, and the absorption column densities agree remarkably well with the *ASCA* measure-

Table 1. *XMM-Newton* GTO observations of RX J0852.0-4622

Rim	Pointing (J2000)		Expos. ksec	XMM revol.
	RA	DEC		
NW	08h48m58s	-45d39m03s	31.76	0252
West	08h47m45s	-46d28m51s	35.96	0252
South	08h53m14s	-47d13m53s	47.13	0253
Center	08h51m50s	-46d18m45s	24.11	0252

Table 2. Spectral fit results with a *wabs(vmekal)+wabs(vmekal+power law)* model for the range $0.2 \leq E_x \leq 10$ keV.

Region	low kT_1 (eV)	high kT_2 (keV)	$N_H(kT_1)$ (10^{22} cm $^{-2}$)	$N_H(kT_2)$ (10^{22} cm $^{-2}$)	power law photon index	χ^2 (dof)	χ^2_ν
NW rim	$37.5^{+4.0}_{-2.0}$	$3.84^{+1.65}_{-1.30}$	$0.138^{+0.022}_{-0.026}$	$0.461^{+0.023}_{-0.019}$	$2.59^{+0.16}_{-0.07}$	796.48 (777)	1.025
Southern rim 1	43.5 ± 0.8	2.92 ± 2.50	0.123 ± 0.016	0.471 ± 0.035	2.55 ± 0.25	349.01 (379)	0.92

ments (Tsunemi et al. 2000, Slane et al. 2001) despite the significantly higher photon statistics and higher energies covered by *XMM-Newton*.

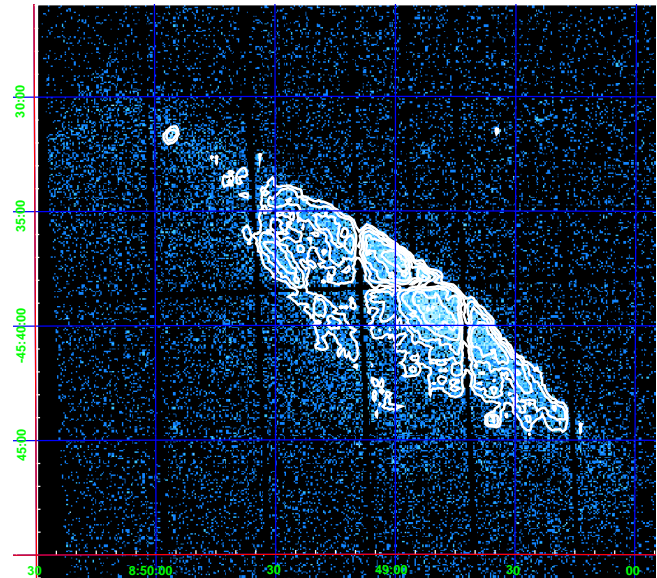
Because of the ambiguity concerning the contribution of the Vela SNR we restricted in what follows the energy range for the fits to $E > 0.8$ keV, which is our third approach to model the spectra.

3.1. The north-western rim

Figure 3 shows the *XMM-Newton* EPIC-PN image of the north-western rim. A bright filament like structure defines the outer edge of the remnant and a second, non-aligned and significantly fainter filament like structure is seen further inside. The two structures seem to join each other at the north-eastern tip. This is actually the first X-ray image which resolves the remnant's outer boundary.

In an attempt to improve upon the non-thermal component modelling of the spectrum with a straight power law model, we have tried in addition the synchrotron model (*sresc*) of XSPEC, developed by Reynolds (1996, 1998). This model represents synchrotron emission from the shock wave accelerated high-energy electrons and which takes care of electron escape or synchrotron losses by a steepening of the spectrum towards higher energies. As can be seen from Table 3 the reduced χ^2_ν value is slightly lower than for a straight power law. As Figure 4 shows two local residuals around ~ 4.4 keV and ~ 6.5 keV are left from the fit. By adding one or two Gaussian shaped line(s) *gauss* at these energies to the *sresc* continuum model it is possible to further lower χ^2_ν (Table 3). We note that a simple power law model is quite acceptable judging on the total χ^2 value. We also note that we still need a thermal component to cover the low energies which is represented by a *vmekal* model

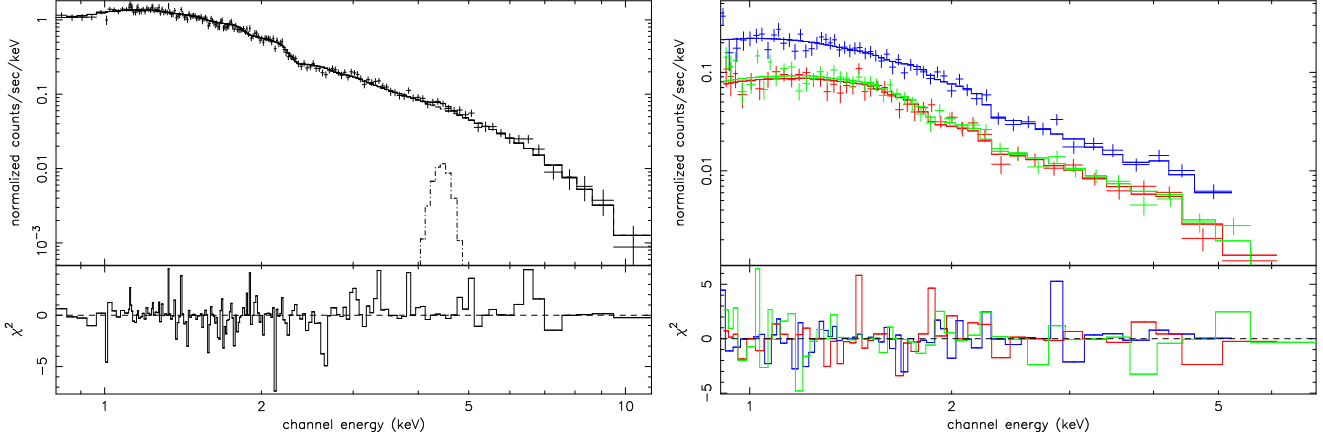
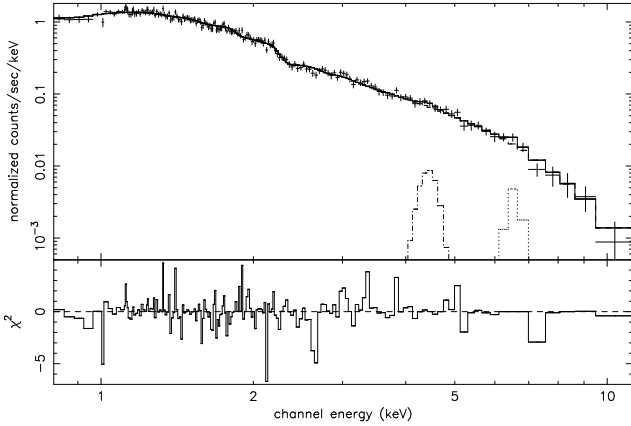
We have also analysed the X-ray spectrum of each of the two filaments (c.f. Fig. 3) separately. Both filaments have a power law continuum spectrum for $E_x \geq 0.8$ keV, which can be also well fitted by the *sresc* model of XSPEC (c.f. Fig. 5).

**Fig. 3.** The *XMM-Newton* EPIC-PN image of the bright NW part of the RX J0852.0-4622 shell, which is spatially resolved for the first time.

The line feature at ~ 4.2 keV detected by *ASCA* (Tsunemi et al. 2000), is also detected by *XMM-Newton* (Iyudin et al. 2004), and is present in both filaments. The line flux is larger in the brighter (outer) filament. Unfortunately, low statistics preclude a reasonable analysis of the line flux radial dependence. We believe that the X-ray line at ~ 4.2 keV is a direct consequence of the ^{44}Ti decay in the SNR shell. Note the sharp outer boundary of the remnant and the clear presence of two arc-like features. The fainter one might correspond to the reverse shock, that only starts to develop. We have detected two line-like excesses, one of which is also visible in the spectrum of the southern rim (see below). The strongest line is at $E_{\text{line}} = 4.24^{+0.18}_{-0.14}$ keV for the NW reg. 1 for a power law continuum model, and $E_{\text{line}} = 4.44 \pm 0.11$ keV for the same region using the *sresc* model. Our values of the line energy are slightly higher than the value given by Tsunemi et al. (2000), but are consistent with

Table 3. Fit results for $E_x \geq 0.8$ keV with various spectral models for the continuum including a power law, the *sresc* model with and without one or two Gaussian lines.

Region	Model	ph. index, or ν_{rolloff} , Hz	N_H (10^{22} cm $^{-2}$)	radio index α at 1 GHz	χ^2 (dof)	χ^2_ν
NW rim	<i>powerlaw</i>	2.60	0.496	—	166.64 (173)	0.963
NW rim	<i>sresc</i>	$(2.2^{+0.4}_{-0.2}) \times 10^{17}$	0.389	0.24	157.76 (172)	0.917
NW rim	<i>sresc+gauss</i>	2.20×10^{17}	0.389	0.24	147.06 (170)	0.865
NW rim	<i>sresc+2gauss</i>	2.20×10^{17}	0.389	0.24	145.04 (170)	0.853
Southern rim	<i>sresc</i>	$(2.6^{+0.6}_{-0.4}) \times 10^{17}$	0.414	0.31	230.707 (225)	1.025

**Fig. 5.** Left: PN spectrum of the brightest region of the RX J0852.0-4622 NW rim (region 1). Right: EPIC-PN and EPIC-MOS1,2 spectra of fainter filament of the NW rim (region 2). Spectra were fitted for $E > 0.8$ keV with the *vmekal+sresc+gauss* model.**Fig. 4.** PN spectrum of the brightest region of the north-western rim of RX J0852.0-4622 for $E > 0.8$ keV in comparison with a *sresc+2 gauss* model fit.

the *ASCA* SIS spectrum of the NW rim (Fig. 4 in the paper of Tsunemi et al. 2000).

Assuming that the line feature is a blend of the hydrogen- and He-like lines of Ca, and that all the Ca consists of ^{44}Ca , we expected to detect a flux of $\sim 5.6 \times 10^{-6}$ ph cm $^{-2}$ s $^{-1}$ from the whole SNR RX J0852.0-4622, based on the flux of $(3.8 \pm 0.7) \times 10^{-5}$ ph cm $^{-2}$ s $^{-1}$ of the line at 1.157 MeV from the ^{44}Ti decay (Iyudin et al. 1998). The significance of the line detection taking exposure and background into account corresponds to $\sim 4 \sigma$ for the whole NW rim. A higher significance is

actually not expected given the 1.157 MeV flux quoted above. The detection of a line with *ASCA* at ~ 4.1 keV is therefore confirmed by the *XMM-Newton* GTO measurements, but the significance is still inconclusive to claim the existence of the line beyond any doubt, although the near coincidence of the line energies is rather compelling.

3.2. The southern rim

The EPIC-MOS1 image of the southern rim of RX J0852.0-4622 is shown in Figure 6.

PN and MOS1,2 spectra have been created for the counts of the region enclosed by the large black ellipse (region 1) and are shown in Figure 7. Again, an emission line like excess at ~ 4.2 keV appears in the spectra. The spectra (Fig. 7) show that both cameras EPIC-PN and EPIC-MOS1,2 detect the line at the same energy and at the same flux level within the flux uncertainties. The right-hand spectrum of Fig. 7 shows that the line energy is the same for different regions (NW and S rims) of the RX J0852.0-4622 shell. The continuum is best fitted by the *sresc* model, but is consistent also with a power law fit (see for more details Iyudin et al. 2004). To illustrate the line excess Figure 8 shows a section of the spectrum between 3 and 6 keV; the left-hand spectrum shows the fit without a line whereas the fit shown in the right-hand side spectrum includes an emission line.

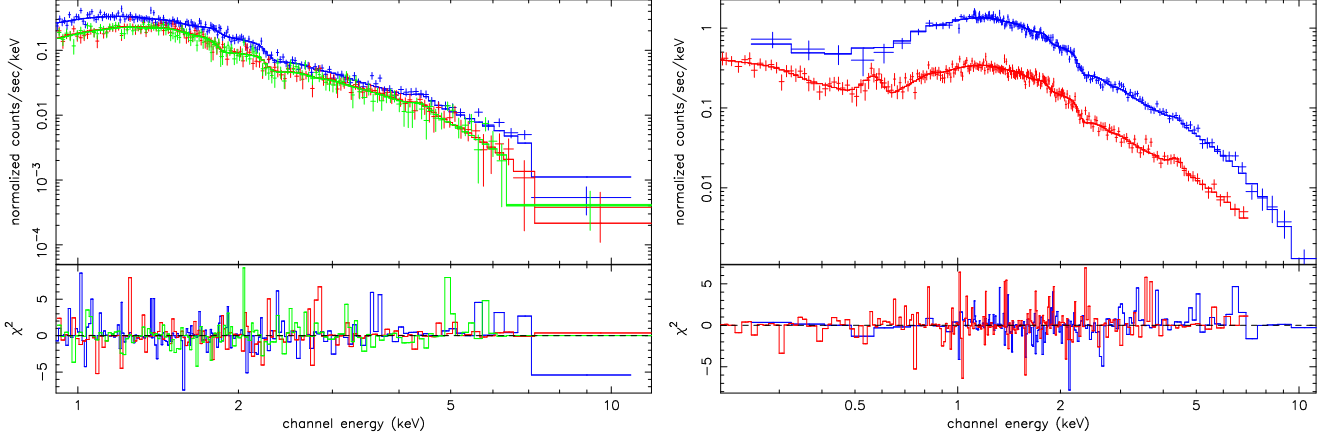


Fig. 7. Left: EPIC-PN and EPIC-MOS1,2 spectra of the RX J0852.0-4622 southern rim brightest region 1 for $E > 0.8$ keV. Right: EPIC-PN spectra of the north-western rim (top curve) and of the southern rim (bottom curve) for $E > 0.2$ keV, in comparison. Spectra were fitted with a *vmekal+sresc+gauss* model.

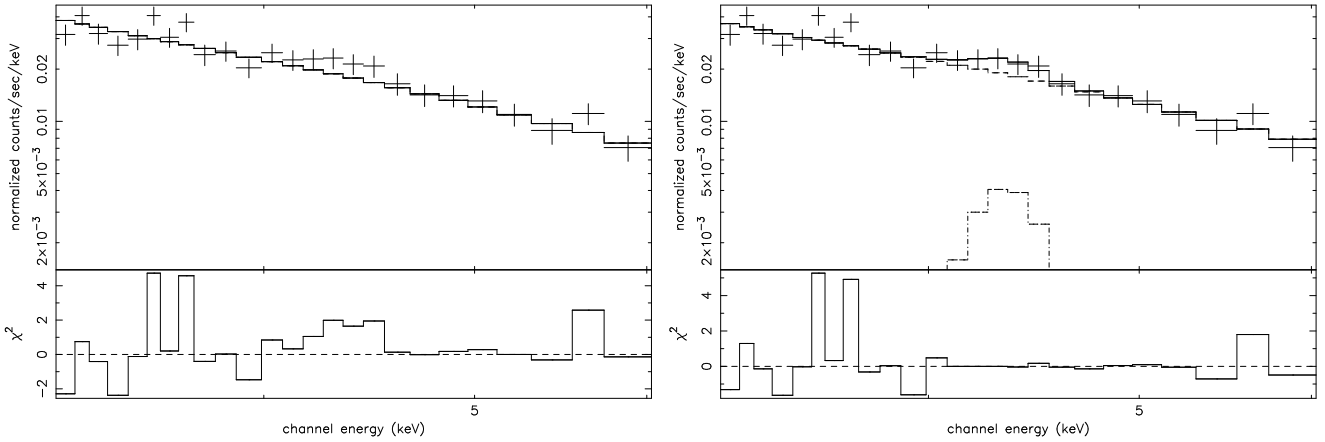


Fig. 8. EPIC-PN spectrum of the RX J0852.0-4622 southern rim brightest region 1 for $3.0 < E < 6.0$ keV; left: *sresc* model fit, right: the same spectrum fitted with a *sresc+gauss* model.

3.3. The western rim

While the NW rim spectra are quite distinct from the underlying thermal emission of the Vela SNR that is dominating at $E_x \leq 0.8$ keV, the western rim spectra for $E_x \geq 0.8$ keV show apart from a steep power law component with a photon index of ~ 4.7 an additional thermal component, which is characterized by $N_H \sim (2.84 \pm 0.15) \times 10^{21} \text{ cm}^{-2}$ and $kT \sim 0.2$ keV. Both the power law and the thermal component are significantly different from those of the NW and S rim. We note that the PN observation of the W rim was heavily contaminated by solar proton flare events that lowered the effective exposure by a factor of three when the *good time interval* selection process was applied. The MOS spectra were not strongly affected by the soft protons and confirm the line emission at 4.4 ± 0.18 keV, also for the western rim.

The western limb shows up in the X-ray image of ROSAT as the X-ray bright feature W (Fig. 1). We note that the radio emission from this part of RX J0852.0-4622 at 2420 MHz is rather weak. This low radio-continuum emission is consistent with the fit to the X-ray spectrum (Fig. 9), which reveals a rel-

atively small contribution of the synchrotron radiation in this region of the SNR.

4. Discussion

4.1. Production mechanisms for the 4.2 keV emission line

The emission line feature at ~ 4.2 keV found by *ASCA* in the NW rim spectrum of RX J0852.0-4622 is also found in the *XMM-Newton* data (Fig. 4, 5, 7, 8 and 9). We have detected two line-like excesses for $E > 4$ keV in the region 1 of the NW rim (Fig. 4), but only one of these lines is visible in the spectra of the western and southern rims. This strongest line is at $E_{line} = 4.24^{+0.18}_{-0.14}$ keV for the NW reg. 1 for a *power law* continuum model, and $E_{line} = 4.44 \pm 0.11$ keV for the same region using the *sresc* model. The spectra of the western and southern rim show the line as well, at an energy which is consistent with that of the NW rim. Our values of the line energy are slightly higher than the value given by Tsunemi et al. (2000), but are consistent with the *ASCA* SIS spectrum of the NW rim (Fig. 4

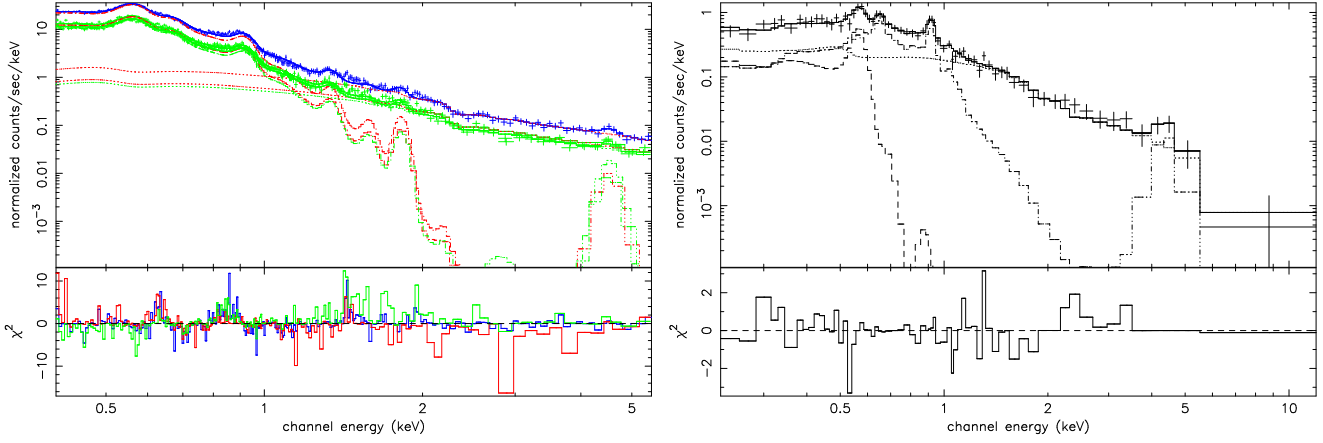


Fig. 9. Left: EPIC-PN spectra of the RX J0852.0-4622 western rim brightest regions, for $E > 0.4$ keV. Right: EPIC-MOS1 spectrum of the western rim region, that overlaps with the brightest regions of the EPIC-PN source region. Spectra were fitted with the $2vmekal+powerlaw+gauss$ model.

Table 4. Line feature parameters derived from the XMM spectra of the SNR rims.

Region	Obs ID	EPIC	Model	E_{line}	$F_{line}, 10^{-6}$	N_H
				keV	$\text{ph cm}^{-2} \text{s}^{-1}$	$(10^{21} \text{ cm}^{-2})$
NW rg1	0112870301	PN	<i>plaw+vmek</i>	$4.24^{+0.18}_{-0.14}$	$3.8^{+3.5}_{-2.8}$	5.0
NW rg1	0112870301	PN	<i>sresc</i>	4.44 ± 0.11	$4.24^{+3.3}_{-3.2}$	3.9
NW rg2	0112870301	PN	<i>sresc</i>	4.2 ± 0.2	$2.4^{+2.7}_{-1.5}$	3.2
South	0112870501	PN	<i>sresc</i>	4.34 ± 0.09	$2.14^{+2.6}_{-1.4}$	4.1
West	0112870401	PN	<i>sresc</i>	4.54 ± 0.07	$9.5^{+8.0}_{-5.0}$	2.8
West	0112870401	MOS1	<i>sresc</i>	4.43 ± 0.18	$26.0^{+14.0}_{-14.0}$	2.6

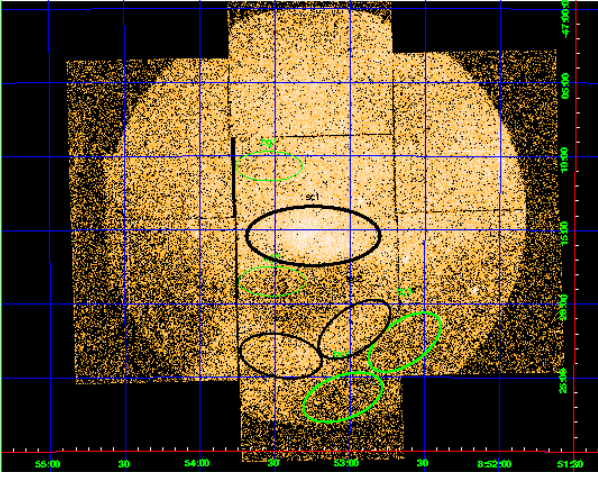


Fig. 6. The *XMM-Newton* EPIC-MOS image of the bright southern part of the RX J0852.0-4622 shell. The black ellipse shows the extraction region for the source spectrum. Green ellipses show the regions from where the background spectra were taken.

in the paper by Tsunemi et al. 2000). The line energies measured with *XMM-Newton* are summarized in Table 4.

The complete data set of lines is consistent with one value for the line energy common to all three sections of the rim, which is $E_x = 4.45 \pm 0.05$ keV.

This line energy can be used for the ion transition identification. From the literature we have found that the closest line is the Ly- β line of H-like Sc, and the next nearest line is the Ly- α line of Ti (see Table 5, Deslattes et al. 2003 and references therein).

It is still possible that the line is the He-like Sc line shifted to higher energy if the line has been produced in ion-atom collisions and has a few satellites (Watson et al. 1974). Depending on the line identification one can consider different production mechanisms.

Assuming that the detected line is a H- or He-like line of ^{44}Sc , that is produced via the ^{44}Ti decay by electron capture, we expect to detect a flux of $\sim 7.2 \times 10^{-6} \text{ ph cm}^{-2} \text{ s}^{-1}$ from the whole SNR, based on the flux of $(3.8 \pm 0.7) \times 10^{-5} \text{ ph cm}^{-2} \text{ s}^{-1}$ of the line at 1.157 MeV from the ^{44}Ti decay (Iyudin et al. 1998). In fact we have detected a total line flux summed over the three X-ray brightest rim sections of $\sim 1.83 \times 10^{-5} \text{ ph cm}^{-2} \text{ s}^{-1}$, which exceeds the expected flux but by less than 2 σ with respect to the measured EPIC-PN flux values and their uncertainties (see Table 4).

The electron loss or capture processes by ions moving in dilute gases are well studied (Betz 1972). The equilibrium charge distribution of the SNR shell ions can be calculated based on the available information about the element abundances in the SNR shell and those of the ISM. One can use the semi-empirical relations of Betz (1972) to compute the mean charge of ions moving in gases. Taking just two values for the expan-

Table 5. Positions, relative intensities of lines and K-shell fluorescent yields of the abundant elements expected for the SNR RX J0852.0-4622 outer shell.

Element	Transition	E_x^1 , (keV)	E_x^2 , (keV)	E_x^3 , (keV)	E_x^4 , (keV)	Relative intensities ¹	ω_K^5 , recommended ⁵
²² Ti	Ly α_2	4.5035	4.5049	4.50486	4.504	0.339±0.040	0.219±0.018
	Ly α_1	4.5097	4.5109	4.51084	4.510	0.661±0.020	
	Ly $\beta_{1,3}$	4.927	4.932	4.93181	4.931	0.248±0.032	
²¹ Sc	Ly α_2	—	—	4.0861	4.085	~0.34	0.190±0.016
	Ly α_1	—	—	4.0906	4.090	~0.66	
	Ly $\beta_{1,3}$	—	—	4.4605	4.460	~0.15	
²⁰ Ca	Ly α_2	3.6890	3.6881	3.68809	3.687	0.34±0.04	0.163±0.016
	Ly α_1	3.6900	3.6917	3.69168	3.691	0.66±0.02	
	Ly $\beta_{1,3}$	4.0123	4.0125	4.0127	4.012	0.103±0.020	

¹ - Verma (2000), ² - Sevier (1979), ³ - Bearden (1967), ⁴ - Johnson & White (1970), ⁵ - Bambynek et al. (1972), the upper left indices attached to the element names in the most left-hand column corresponds to the nuclear charge.

sion velocity of the SNR shell, i.e. $\sim 5,000$ km/s or $15,300$ km/s (Iyudin et al. 1998) one can derive from the empirical relation of Fig. 5.11 of Betz (1972) the mean charge of the Sc ions which move with the SNR shell to $\langle q \rangle \sim 4.4$ and ~ 13.2 , respectively. To describe the charge distribution of the ions moving in dilute gaseous matter we use the approach of Nikolaev (1965) and of Betz (1972) again. In the first approximation the experimentally derived equilibrium charge distribution of ions in gaseous matter is well described by a Gaussian with the r.m.s. value d that can be expressed as $d = 0.27Z^{1/2}$, and by the mean charge of all ions of a particular element of nuclear charge Z . The equilibrium charge distribution can be written as

$$F_q \approx (2\pi d^2)^{-1/2} \exp[-(q - \langle q \rangle)^2 / 2d^2]. \quad (1)$$

From this Gaussian distribution it is obvious that even for the highest derived expansion velocity of the SNR shell (Iyudin et al. 1998) the equilibrium charge distributions of ⁴⁴Ti and the ⁴⁴Sc will be limited to the range of charges ≤ 16 with a probability of $\sim 99\%$. For solar abundances of the ISM the influence of the known asymmetry in the equilibrium charge distribution created by high Z gas mixtures has a minor effect as far as the extension of the charge distribution towards higher ionization states is concerned. For the target gas consisting mainly of hydrogen and helium the equilibrium charge distribution remains Gaussian (symmetric) (Betz 1972). It means that without invoking other inner-shell ionization mechanisms we should not have hydrogen- or helium-like transitions in Sc or Ti in the SNR shell.

Note that the situation is completely different for the Cas A SNR where thermal processes dominate the formation of the charge distribution, in contrast to the case of RX J0852.0-4622 where the reverse shock is likely to be still very weak (Iyudin & Aschenbach 2001).

4.2. Charge states of the abundant ions in the outer rim

To estimate the line flux two hypotheses for the origin seem plausible at this point in time, i.e., (1) - the line is the result of inner-shell ionization of the abundant constituents of the SNR

rim induced by electron capture decay, or (2) - the line is a consequence of collisions of ions present in the SNR outer shell with the ambient matter, predominantly with the ISM hydrogen atoms or electrons. In the latter case the width and the shift of the line are carrying information about the expansion velocity of the SNR (Moore et al. 1972, Kauffman et al. 1973, Garcia et al. 1973, Verma 2000, Iyudin and Aschenbach 2001). Most likely the line at ~ 4.4 keV is a blend of lines emitted by ⁴⁴Sc after ⁴⁴Ti decay. But one cannot a priori exclude the possibility that at least part of the line flux is produced via the inner-shell ionization of Ti induced by collisions with ambient matter.

Two Ti isotopes are abundantly produced and transported to the outer layers of the sub-Chandrasekhar type Ia SNe ejecta, which are ⁴⁴Ti and ⁴⁸Ti, the latter is originally produced as ⁴⁸Cr in quantities comparable to ⁴⁴Ti (Livne & Arnett 1995, Woosley & Weaver, 1994). Interestingly, ⁴⁸Cr decays via electron capture (100%) to ⁴⁸V, which in turn decays to ⁴⁸Ti via electron capture (50.4%) and β^+ decay (49.6%). This sequence will eventually leave the ⁴⁸Ti isotope also in ionized and excited states. The life-times of ⁴⁸Cr and ⁴⁸V are 21.56 hr and 15.976 days, respectively. Therefore, the K-shell X-ray transitions following the Cr and V decays via electron capture have happened long ago, and no bright X-ray lines are expected from these two isotopes unless further inner-shell vacancies are generated by ion interactions with the ISM. The consequence of the K-shell vacancies after the inner-shell ionization in the collisions with the ambient atoms is that predominantly K- α and/or K- β lines of Ca and Ti are emitted, with relative line strengths of K- α and K- β given by the corresponding fluorescence yields (c.f. Table 5).

The scenarios introduced above can also serve to answer questions about the exclusive inner-shell ionization of just Sc and Ti. Given the X-ray brightness distribution of RX J0852.0-4622 it seems that this SNR only has started to interact with denser ISM matter at the north-western and southern boundaries, if at all. There is no clear indication of the existence of a reverse shock, which would be the consequence of such an interaction. Only the presence of the two filament-like structures in the north-western section may be taken as evidence for a reverse shock and if so it only recently has started to de-

velop. If RX J0852.0-4622 is indeed young (Iyudin et al. 1998, Aschenbach et al. 1999), then its expansion velocity can still be as high as indicated by the width of the γ -ray line (Iyudin et al. 1998), e.g. $V_{exp} \sim 15.000 \text{ km s}^{-1}$. In this case ions contained in the outermost layers of the ejecta will have kinetic energies of $\sim 1 \text{ MeV/amu}$, and therefore will experience internal ionisation of the K-shell through collisions with the heavy atoms (ions) of the ambient matter, possibly contained in clouds. As a result of such an interaction also the emitted K- α and K- β lines of Sc and Ti could be broadened and shifted to higher energies because of the contribution of satellite lines created in these heavy ion-atom collisions (Moore et al. 1972, Kaufmann et al. 1973, Whalen & Briancon 1975). But such an interpretation seems to be in conflict with measured position, shape and energy spread of the X-ray lines.

The lines detected by the *XMM-Newton* EPIC-PN camera in each of the observed three sections of the SNR seem to be slightly broadened with an r.m.s. width of 150 eV, that has to be compared with the instrumental energy resolution of $\leq 125 \text{ eV}$ at the appropriate energy of 4.4 keV (EPIC-PN, Haberl et al. 2002). The natural widths of the K- α lines of elements with $Z \sim 20$ are $\leq 2 \text{ eV}$ (Krause & Oliver 1979). The energy shift of the line position depends on the projectile type and its kinetic energy (Moore et al. 1972, Kauffman et al. 1973, Verma 2000), and has a maximum value of $\sim 80 \text{ eV}$ for Ti (Moore et al. 1972, Verma 2000). But an energy shift of the detected line cannot be unambiguously claimed from the data. Instead, we believe that the line position is consistent with the unshifted K- β line of Sc. At last the line broadening of $\sim 80 \text{ eV}$ could be produced by Doppler motion, that would lead to a radial projected average velocity of the emitting volume of the order of $\sim 5800 \text{ km/s}$. This value for the expansion velocity of RX J0852.0-4622 is lower than the value derived from the broadening of the line at 1.157 MeV (Iyudin et al. 1998). But this X-ray derived value may not be in a conflict with the γ -ray derived velocity, given the possibility that the geometry and the velocity of the emitting volume elements need not to be the same.

4.3. GRO J0852-4642 spectrum and progenitor

In the following section we take the view that the measurements of ^{44}Ti with *COMPTEL* are real and not a statistical excursion in the spectrum (Iyudin et al. 1998). Both the *ASCA* and the *XMM-Newton* measurements of the 4.4 keV emission feature support this interpretation, and we use this information to access the type of progenitor of RX J0852.0-4622 / GRO J0852-4642. ^{44}Ti is believed to be synthesized near the mass cut interface in core-collapse SNe explosions (Woosley and Weaver 1995, Timmes et al. 1996). Therefore, the total yield and spatial distribution of ^{44}Ti produced in such an explosion are very sensitive to the explosion mechanism and the ejecta dynamics, e.g. in SNe of type Ia a mass cut does not exist. Assuming that the ^{44}Ti line profile measurements by *COMPTEL* (Iyudin et al. 1998) are not far from reality, which is supported by comparison with the ^{26}Al line shape derived for the same instrument (see Fig. 2 in Iyudin et al. 1998), we need to understand expansion velocities of $15300 \pm 3700 \text{ km}$

s^{-1} for ^{44}Ti , and $\leq 8000 \text{ km s}^{-1}$ for ^{26}Al . We compare the measurements of both the expansion velocity and the abundances of Ca and Ti with the model predictions of Woosley and Weaver (1994) and Livne and Arnett (1995). It turns out that our measurements are only met by models for a sub-Chandrasekhar type Ia supernova explosion. This means that the progenitor of RX J0852.0-4622 was very likely a 0.6-0.7 M_{\odot} helium accreting white dwarf and according to present knowledge no compact remnant is expected to be associated with RX J0852.0-4622. Of course we are then left with the question about the nature and origin of the central point-like source CXOU J085201.4-461753. Clearly, the ionization state of the Ti can have an impact on the above conclusion but of moderate size. For example, values of age and distance to the SNR may be underestimated, but not more than by $\sim 30\%$ (Aschenbach et al. 1999). Mochizuki et al. (1999) have modelled the heating and ionization of ^{44}Ti by the reverse shock in Cas A, for which they report the possibility of a currently increased ^{44}Ti activity. With respect to RX J0852.0-4622 / GRO J0852-4642 they find that the reverse shock does not heat the ejecta to sufficiently high temperatures to ionize ^{44}Ti because of the low ambient matter density.

5. Conclusion

XMM-Newton observations of three sections on the rim of RX J0852.0-4622 have been carried out. The north-western rim has been resolved in two clearly separated filament-like structures. The high energy section of the spectra of both the north-western rim and the southern rim are consistent with a power law shape and a power law which shows a roll-off towards high energies. Interestingly, the roll-off energy of about 1 keV is fairly high and it remains an open question what the spectrum looks like towards lower energies. The difficulty here is the contribution from the Vela SNR, which is fairly bright at energies below 1 keV. The various models seem to verify an absorbing column density towards RX J0852.0-4622 which is significantly higher than typical for the Vela SNR. Whether this implies a greater distance is not clear. The spectral slope measured with *XMM-Newton* is basically the same as what has been measured with *ASCA*. The western part of the remnant is different as it shows only a small contribution by a power law and if present at all the spectrum is much steeper. The *ASCA* measurements indicated the presence of an emission line like feature at around 4.1 - 4.2 keV. The *XMM-Newton* data confirm such a feature, and it seems to be present everywhere on the remnant's rim. The line energy averaged over the three observational fields is $4.45 \pm 0.05 \text{ keV}$. We attribute this line or lines to the emission of Ti and Sc which might be excited by atom/ion or ion/ion collisions. The X-ray line flux expected from such an interaction is consistent with the 1.157 MeV γ -ray line flux measured by *COMPTEL*. This consistency of the X-ray line flux and the γ -ray line flux lends further support to the existence and amounts of Ti in RX J0852.0-4622 claimed by Iyudin et al. (1998) and to the suggestion that RX J0852.0-4622 is young and nearby (Aschenbach et al. 1999). Iyudin et al. (1998) quote a very large broadening of the 1.157 MeV γ -ray line which would indicate a large velocity of the emit-

ting matter of about 15.000 km/s. Such a high ejecta velocity for Ti is found only in explosion models of sub-Chandrasekhar type Ia supernovae (Woosley & Weaver 1994, Livne & Arnett 1995). In this case no compact remnant is expected. The obvious questions remaining are what the nature and the origin of the central compact source CXOU J085201.4-461753 are and why the absorption column density apparently associated with RX J0852.0-4622 is much greater than typical for Vela.

6. Acknowledgements

The authors acknowledge the comments of the anonymous referee that helped to improve the quality of the paper. The XMM-Newton project is an ESA Science Mission with instruments and contributions directly funded by ESA Member States and the USA (NASA). The XMM-Newton project is supported by the Bundesministerium für Bildung und Forschung / Deutsches Zentrum für Luft- und Raumfahrt (BMBF / DLR), the Max-Planck-Gesellschaft and the Heidenhain-Stiftung. The COMPTEL project was supported by the BMBF through DLR grant 50 QV 9096 8. AFI acknowledges financial support from the BMBF through the DLR grant 50 OR 0002.

References

- Aschenbach B. 1998, *Nature* 396, 141
- Aschenbach, B., Iyudin, A. F., Schönfelder, V. 1999, *A&A*, 350, 997
- Bambyneck, W., Crasemann, B., Fink, R. W., et al. 1972, *Rev. Mod. Phys.*, 44, 716
- Bearden, J. A. 1967, *Rev. Mod. Phys.*, 39, 78
- Betz, H.-D. 1972, *Rev. Mod. Phys.*, 44, 465
- Burgess, C. P., & Zuber, K. 2000, *Aph*, 14, 1
- Cha, A. N., Sembach, K. R., Danks, A. C. 1999, *ApJ*, 515, 25
- Cha, A. N., & Sembach, K. R. 2000, *ApJS*, 126, 399
- Combi, J. A., Romero, G. E., Benaglia, P. 1999, *ApJ*, 519, L177
- Deslattes, R. D., Kessler, E. G., Jr., Indelicato, P., et al. 2003, *Rev. Mod. Phys.*, 75, 35
- Duncan, A. R., and Green, D. A. 2000, *A&A*, 364, 732
- Filipovic, M. D. 2001, private communication
- Garcia, J. D., Fortner, R. J., Kavanagh, T. M. 1973, *Rev. Mod. Phys.*, 45, 111
- Haberl, F., Briel, U., Dennerl, K., and Zavlin, V. E. 2002, *astro-ph/0203235*
- Iyudin, A. F., Diehl, R., Bloemen, H., et al. 1994, *A&A*, 284, L1
- Iyudin, A. F., Diehl, R., Lichti, G. G., et al. 1997, *ESA-SP382*, 37
- Iyudin, A. F., Schönfelder, V., Bennett, K., et al. 1998, *Nature*, 396, 142
- Iyudin, A. F. 1999, *Nucl. Physics*, A654, 900c
- Iyudin, A. F. 2000, *Proc. of Workshop Astronomy with Radioactivities, Schloss Ringberg, Kreuth, Germany, September 29 - October 2, 1999*, MPE Report, 274, 65
- Iyudin, A. F., & Aschenbach, B. 2001, *ASP CS-251*, 28
- Iyudin, A. F., Aschenbach, B., Haberl, F., et al. 2004, *ESA SP-488*, in print
- Johnson, G. G., Jr., & White, E. W. 1970, *ASTM Data Series DC46*
- Kargaltsev, O., Pavlov, G. G., Sanwal, D., Garmire, G. P. 2002, *ApJ*, 580, 1060
- Kauffman, R. L., McGuire, J. H., Richard, P. 1973, *Phys. Rev.*, A8, 1233
- Krause, M. O., & Oliver, J. H. 1979, *J. Phys. Chem. Ref. Data*, 8, 329
- Livne, E., Arnett, D. 1995, *ApJ*, 452, 62
- Lu, F. J. & Aschenbach, B. 2000, *A&A*, 362, 1083
- Mereghetti, S., Pellizzoni, A., de Luca, A. 2002, *ASP CS-271*, 289
- Mochizuki Y., Takahashi K., Janka H.-Th., Hillebrandt W., Diehl R. 1999, *A&A* 346, 831
- Moore, C. F., Senglaub, M., Johnson, B., Richard, P. 1972, *Phys. Let.*, 40A, 107
- Nikolaev, V. S. 1965, *Usp. Fiz. Nauk* 85, 679 [*Sov. Phys. Usp.*, 8, 269 (1965)]
- Pavlov, G., Sanwal, D., Kiziltan, B., Garmire, G. P., et al. 2001, *ApJ*, 559, L131
- Pozzo, M., Jeffries, R. D., Naylor, T., et al. 2000, *MNRAS*, 313, L23
- Redman, M. P., Meaburn, J., Bryce, M., Harman, D. J., & O'Brien, T. J. 2002, *MNRAS*, 336, 1093
- Reynolds, S. P. 1996, *ApJ*, 459, L13
- Reynolds, S. P. 1998, *ApJ*, 493, 375
- Schönfelder, V., Bloemen, H., Collmar, W., et al. 2000, *AIP Conf. Proc.* AIP, 510, 54
- Sevier, K. D. 1979, *At. Data Nucl. Data Tables*, 24, 323
- Slane, P., Hughes, J. P., Edgar, R. J., et al. 2001, *ApJ*, 548, 814
- Strüder, L., Briel, U., Dennerl, K., et al. 2001, *A&A*, 365, L18
- Timmes, F. X., Woosley, S. E., Hartmann, D. H., & Hoffman R. D. 1996, *ApJ* 464, 332
- Tsunemi H., Miyata E., Aschenbach B., Hiraga J., & Akutsu D. 2000, *PASJ* 52, 887
- Turner, M. J. L., Abbey, A., Arnaud, M., et al. 2001, *A&A*, 365, L27
- Verma, H. R. 2000, *J. Phys.*, B33, 3407
- Vink, J., Laming, J. M., Kaastra, J. S., et al. 2001, *ApJ*, 560, L79
- von Kienlin, A., Attié, D., Schanne, S., et al. *Proc. of the 5th INTEGRAL Workshop The INTEGRAL Universe, Munich, 16-20 February 2004, ESA SP-552, accepted, astro-ph/0407129*
- Wang, C.-Y. & Chevalier, R. A. 2002, *ApJ*, 574, 155
- Watson, R. L., Jenson, F. E., Chiao, T. 1974, *Phys. Rev.*, A10, 1230
- Whalen, R. J., & Briancon, C. 1975, in *Atomic Inner-Shell Processes*, ed. B. Crasemann, 2, 233
- Woermann, B., Gaylard, M. J., & Otrupcek, R. 2001, *MNRAS*, 325, 1213
- Woosley, S. E., Weaver, T. A. 1994, *ApJ* 423, 371
- Woosley, S. E., Weaver, T. A. 1995, *ApJS* 101, 181
- Zinchenko, I., Mattila, K., & Toriseva, M. 1995, *A&AS*, 111, 95